

SAR and factor IXa crystal structure of a dual inhibitor of factors IXa and Xa

Joanne M. Smallheer,* Richard S. Alexander, Jianmin Wang, Shuaige Wang, Suanne Nakajima, Karen A. Rossi, Angela Smallwood, Frank Barbera, Debra Burdick, Joseph M. Luetttgen, Robert M. Knabb, Ruth R. Wexler and Prabhakar K. Jadhav

Bristol-Myers Squibb Company, PO Box 5400, Princeton, NJ 08543-5400, USA

Received 16 June 2004; revised 16 August 2004; accepted 16 August 2004

Available online 15 September 2004

Abstract—Modifications to the P4 moiety and pyrazole C3 substituent of factor Xa inhibitor **SN-429** provided several new compounds, which are 5–10 nM inhibitors of factor IXa. An X-ray crystal structure of one example complexed to factor IXa shows that these compounds adopt a similar binding mode to that previously observed with pyrazole inhibitors in the factor Xa active site both with regard to how the inhibitor binds and the position of Tyr99.

© 2004 Elsevier Ltd. All rights reserved.

Thromboembolic events such as deep vein thrombosis (DVT), pulmonary embolism, myocardial infarction, and thromboembolic stroke are collectively the major cause of mortality and morbidity in the industrialized world. Normal hemostasis is maintained as the result of a complex interplay among the numerous serine proteases that regulate the process of coagulation. The ideal point of intervention in the coagulation cascade to achieve an optimum combination of efficacy (anticoagulatory effects) and safety (i.e., a low incidence of bleeding) will only be determined after selective inhibitors of the various coagulation serine proteases have been identified and compared in vivo. While significant benefit has been demonstrated in the treatment of deep vein thrombosis using both thrombin and factor Xa inhibitors, in clinical practice one drug/mechanism of action may not be ideal for all antithrombotic indications.¹ Antithrombotic drugs that target the ‘intrinsic’ pathway of clot propagation, as opposed to the ‘extrinsic’ pathway of clot initiation may provide a means of preventing vessel occlusion without blockade of coagulation at an injury site along the vessel wall. In vivo studies with active-site blocked factor IXa or antifactor IXa antibodies have demonstrated that good efficacy in animal

models of arterial and venous thrombosis can be achieved via this mechanism.^{2,3}

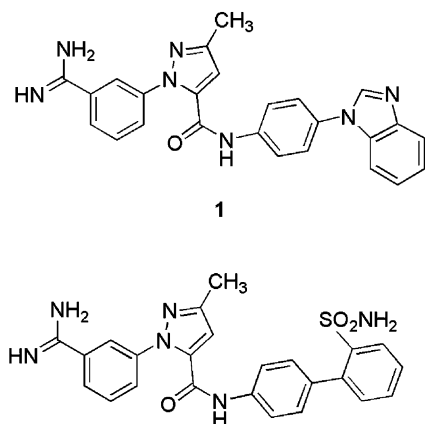
High throughput screening of compounds from our thrombin and factor Xa (fXa) programs yielded a number of potent, but nonselective, factor IXa (fIXa) inhibitors. Specifically, compound **1**, a subnanomolar inhibitor of fXa, was identified as an 82 nM inhibitor of fIXa. In comparison, a structurally similar compound **SN-429**,⁴ a picomolar fXa inhibitor, was only a weak inhibitor of fIXa (Table 1).

This suggested that a re-optimization of the P4 substituent in our existing fXa scaffolds might lead to additional potent and selective fIXa inhibitors. As a result of a two amino acid insertion in the fIXa 99-loop, and the specific interactions of the amino acid side chains in this loop, which are unique to fIXa, the 99-loop in fIXa provides an environment in the S4 binding pocket that should be quite distinct from that of fXa.⁷ The published X-ray crystal structure of porcine fIXa inhibited with an irreversible inhibitor (D)-Phe-Pro-Asp-chloromethylketone (PPACK), which forms a covalent bond to the catalytic serine, shows an unusual orientation of Tyr99, which blocks the S3/S4 binding site and allows binding of proline in the S2 pocket.^{8a} The crystal structure of human fIXa inhibited with *p*-aminobenzamidine also has Tyr99 rotated to partially block access to the S4 pocket.^{8b} In keeping with these observations in the published crystal structures, it has been shown by

Keywords: Factor IXa; Factor Xa; Pyrazole.

*Corresponding author. Tel.: +1 609 818 5332; fax: +1 609 818 3450; e-mail: joanne.smallheer@bms.com

Table 1.



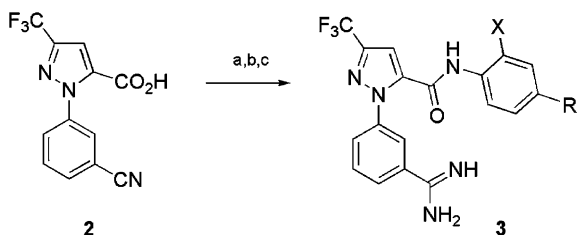
SN-429

Compd	IXa K_i^5 (nM)	Xa K_i^6 (nM)	IXa/Xa
1	82	0.38	216
SN-429	1900	0.013	> 100,000

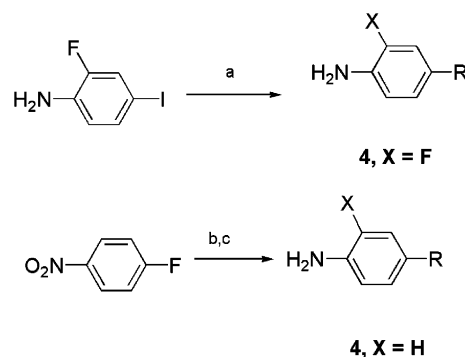
site-directed mutagenesis that the amino acid sequence in the 99-loop of fIXa plays a key role in determining substrate selectivity for small peptide substrates.⁹

It was hoped that additional structural modifications based on the differences in amino acid sequences in other areas of the fIXa and fIXa active sites could then be exploited to introduce additional fIXa potency. In particular, we were interested in targeting an interaction with Glu219, since this residue is unique to fIXa whereas the other coagulation serine proteases all have a conserved glycine residue at this position. It has been postulated that the relatively poor catalytic efficiency of fIXa is due in part to a partial collapse of the S1 recognition pocket, since Glu219 must assume a high energy main chain conformation to accommodate substrate binding.⁷ In the human fIXa-*p*-aminobenzamidide crystal structure, this conformation is stabilized by a salt bridge between the side chains of Glu219 and Arg148.^{8b} A direct interaction between a bound inhibitor and the carboxylic acid of Glu219 might therefore result in increased affinity through stabilization of the inhibitor–enzyme complex.

Scheme 1 shows the preparation of analogs of **1** from pyrazole carboxylic acid **2** using previously described procedures.^{4,10}



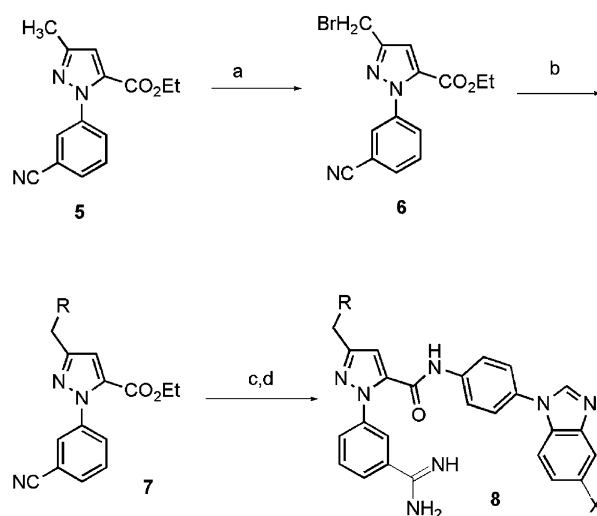
Scheme 1. Reagents and conditions: (a) COCl_2 , DMF, CH_2Cl_2 ; (b) **4**, pyridine, DMAP, CH_2Cl_2 , 50–80%; (c) HCl, MeOH then $(\text{NH}_4)_2\text{CO}_3$, EtOH, 50–70%.



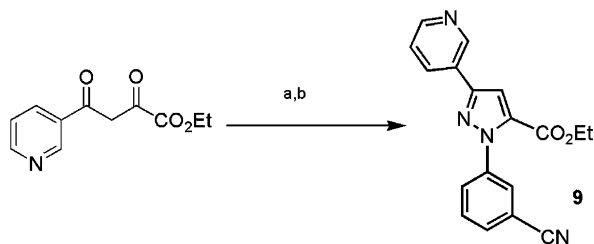
Scheme 2. Reagents and conditions: (a) N-heterocycle, CuI, K_2CO_3 , 1,10 phenanthroline, DMF, 110 °C, 40–60%; (b) N-heterocycle, K_2CO_3 , DMSO, 55–85%; (c) $\text{H}_2/\text{Pd}/\text{MeOH}$, 80–95%.

Anilines **4** with *o*-fluoro-substitution were prepared as illustrated in Scheme 2 by Ullmann coupling of the desired N-heterocycle with 2-fluoro-4-iodoaniline. Des-fluoro anilines were conveniently obtained by direct nucleophilic aromatic substitution of 4-fluoronitrobenzene followed by reduction of the nitro group to the corresponding amine. When the N-heterocycle employed was an unsymmetrically substituted benzimidazole or azabenzimidazole, mixtures of regioisomers were obtained and were separated either by silica gel chromatography at the aniline stage or by reverse phase HPLC after elaboration of the final targets.¹¹

Heterocycles capable of forming ionic interactions or H-bonds to Glu219 were introduced on the methyl group at C3 of the pyrazole ring as shown in Scheme 3. Compound **5**⁴ was brominated by treatment with *N*-bromosuccinimide to give monobromo intermediate **6**, followed by displacement of the bromide with imidazole, triazole, or tetrazole to provide esters **7**, which were condensed with the appropriate aniline **4** using Weinreb conditions. A Pinner reaction followed by ammonolysis provided amidines **8**.



Scheme 3. Reagents and conditions: (a) NBS, CCl_4 , reflux, 35–40%; (b) imidazole, triazole, or tetrazole, K_2CO_3 , DMF, 60–70%; (c) $(\text{CH}_3)_3\text{Al}$, CH_2Cl_2 , **4**, 20–50%; (d) HCl/MeOH then $(\text{NH}_4)_2\text{CO}_3$ /EtOH, 40–60%.



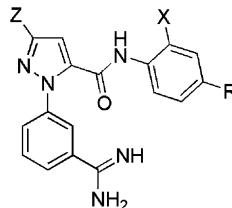
Scheme 4. Reagents and conditions: (a) MeONH₂·HCl, EtOH, sieves, 87%; (b) 3-cyanophenylhydrazine, HOAc, reflux, 68%.

Compounds with a 3-pyridyl ring attached directly to the pyrazole core were prepared from ethyl nicotinoylpyruvate¹² as shown in Scheme 4 by treatment with methoxyamine hydrochloride followed by condensation of the resulting ethyl 2-(methoxyimino)-4-oxo-4-(pyridin-3-yl)butanoate with 3-cyanophenylhydrazine in acetic acid at reflux. This gave a 9:1 mixture in favor of the desired pyrazole regioisomer **9**.¹³ Further elaboration of **9** was carried out as described above for the conversion of **7** to **8**.

Compounds were assayed for inhibitory activity against fIXa and fXa using purified human enzymes by published methods, which measure the inhibition of enzymatic hydrolysis of small peptidic chromogenic substrates.^{5,6} Potency against fIXa, as well as the ratio

of fIXa to fXa potency, was improved by replacement of the C3 pyrazole methyl group in **1** with a trifluoromethyl group in compound **3a**. However, unlike many similar fXa compounds, where an additional modest potency enhancement was realized by the introduction of an *o*-fluoro substitution on the inner phenyl ring,⁴ compound **3b** had comparable fIXa potency and selectivity to **3a**. In the S4 pocket, an additional nitrogen at different positions around the phenyl ring of the benzimidazole in examples **3c–f** had little effect on the fIXa potency, while slightly improving the fXa potency, for an overall detrimental effect of the selectivity for fIXa over fXa. The addition of a 5- or 6-chloro substituent in compounds **3g** and **3h**, however, provided a 2–3-fold improvement in fIXa affinity and significantly improved the ratio of fIXa/fXa potency. Trifluoromethyl compound **3i** had similar potency and selectivity to the chloro compounds whereas methyl, amino, and nitro compounds **3j–l** had potency similar to the unsubstituted benzimidazoles and displayed decreasing selectivity with respect to fXa. The 5,6-dichloro compound **3m** was both less potent and less selective for fIXa compared with either of the monochloro analogs. Replacing the benzimidazole with indole **3n** resulted in loss of potency with respect to both enzymes, while the benzimidazolone analog **3o** was 15-fold less active toward fIXa while maintaining good fXa potency. Truncating the benzimidazole ring to imidazole in **3p** also

Table 2. Analogs of compound **1**



Compd ^a	Z	X	R	IXa K _i (nM) ^b	Xa K _i (nM) ^b	IXa/Xa
1	CH ₃	H	1-Benzimidazolyl	82	0.38	216
3a	CF ₃	H	1-Benzimidazolyl	11	0.094	117
3b	CF ₃	F	1-Benzimidazolyl	13	0.10	130
3c	CF ₃	F	1-(4-Azabenzimidazolyl)	7.9	0.024	329
3d	CF ₃	F	1-(5-Azabenzimidazolyl)	8	0.036	220
3e	CF ₃	F	1-(6-Azabenzimidazolyl)	7.9	0.044	180
3f	CF ₃	F	1-(7-Azabenzimidazolyl)	13	0.028	464
3g	CF ₃	F	1-(5-Chlorobenzimidazolyl)	4.2	0.42	10
3h	CF ₃	F	1-(6-Chlorobenzimidazolyl)	5.1	0.25	20
3i	CF ₃	F	1-(5-Trifluoromethyl-benzimidazolyl)	6.4	0.29	22
3j	CF ₃	F	1-(5-Methylbenzimidazolyl)	10	0.27	37
3k	CF ₃	F	1-(5-Aminobenzimidazolyl)	11	0.12	92
3l	CF ₃	F	1-(5-Nitrobenzimidazolyl)	11	0.08	138
3m	CF ₃	F	1-(5,6-Dichlorobenzimidazolyl)	26	0.27	96
3n	CF ₃	F	1-Indolyl	1700	5.4	283
3o	CF ₃	H	1-(2-Oxobenzimidazolyl)	190	0.058	>3000
3p	CF ₃	H	1-Imidazolyl	72	0.091	791
8a	1-Imidazolylmethyl	H	1-Benzimidazolyl	120	0.58	207
8b	1-(1,2,4-Triazolylmethyl)	H	1-Benzimidazolyl	44	0.19	232
8c	1-(1,2,3-Triazolylmethyl)	H	1-Benzimidazolyl	20	0.26	77
8d	1-Tetrazolylmethyl	H	1-Benzimidazolyl	11	0.31	35
8e	3-Pyridyl	H	1-Benzimidazolyl	5.5	0.20	28
8f	3-Pyridyl	H	1-(5-Chlorobenzimidazolyl)	15	0.65	23

^a All of the compounds in Table 2 were isolated as TFA salts by reverse phase HPLC and gave satisfactory spectral and analytical data.

^b Biological assays were carried out as described in Refs. 5 and 6.

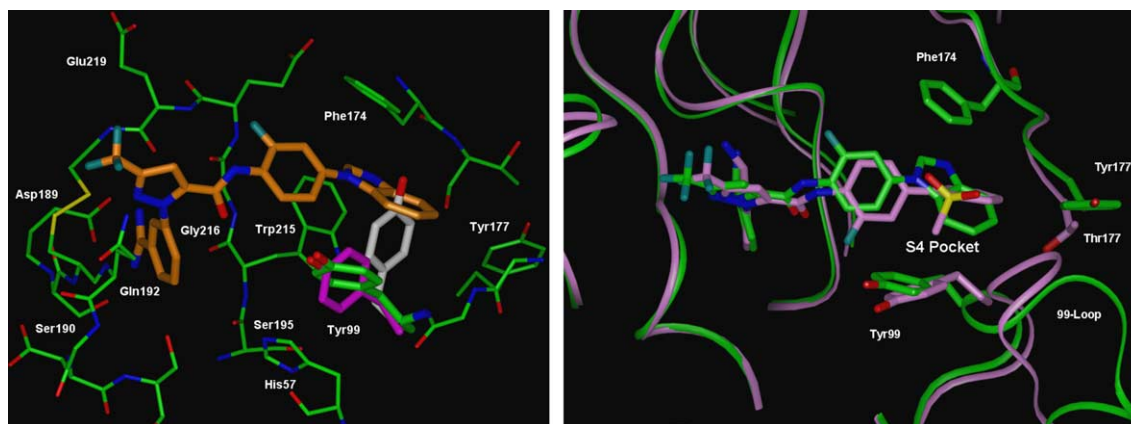


Figure 1. (a) X-ray crystal structure of compound **3b** (in orange) complexed with porcine fIXa (in green). Also shown are the alternate orientations of Tyr99 from the published PPACK-fIXa (in white) and the *p*-aminobenzamidine-fIXa (in magenta) crystal structures. (b) Overlay of the fIXa-**3b** crystal structure (in green) with the DMP-423-fIXa structure (in pink).

decreased fIXa potency without adversely affecting the fXa potency. The best combination of fIXa potency and selectivity in this series was thus obtained with 5-chlorobenzimidazole as the P4 substituent (**3g**).

Substitution of heterocycles at the 3-position of the pyrazole ring to interact with Glu219 did not provide the significant increase in potency or selectivity expected from a strong ionic or H-bonding interaction with the Glu side chain carboxylic acid. The tetrazole **8d** and pyridine **8e** did show improved potency and selectivity as compared to compound **1**, in a similar range to substituted benzimidazoles **3h–j**. Combining the 3-pyridylpyrazole substitution with a 5-chlorobenzimidazole P4 in compound **8f**, however, did not result in additional potency over that observed for either substitution alone. The compounds in Table 2 also showed modest selectivity (5–40-fold) for fIXa over thrombin and trypsin (unpublished results). No in vivo evaluations were carried out on this series of compounds.

The crystal structure of porcine fIXa complexed with compound **3b** is shown in Figure 1a.¹⁴ The inhibitor is anchored into the active site by the bidentate interaction between the benzamidine group and Asp189 of fIXa. A hydrogen bond is observed between N2 of the pyrazole ring and the backbone nitrogen of Gln192. The amide carbonyl is also engaged in a hydrogen bond with the backbone nitrogen of Gly216. The overall binding mode of this inhibitor is quite similar to that observed with reversible fXa inhibitors complexed in fXa^{10,15} in that the inhibitor optimizes interactions in the S1 pocket and S4 region of the protein using a linker that engages in hydrogen bonds with backbone residues of the enzyme. In contrast to the previously published fIXa structures, the fIXa-**3b** structure shows an orientation of the Tyr99 residue that is more consistent with the orientation observed in fXa crystal structures and that accommodates binding of the inhibitor in the S4 pocket, such that the benzimidazole-phenyl group is situated in the hydrophobic box surrounded by residues Trp215, Tyr99, and Phe174.

Figure 1b shows the overlay of the fIXa-**3b** crystal structure with the crystal structure of DMP423, a potent and selective fXa inhibitor, complexed with fXa.¹⁰ With the exception of the area of the 99-loop, the backbones of the two enzymes are very similar, and the two inhibitors bind in the active sites in essentially the same way. In both crystal structures, Tyr99 blocks the S2 pocket and forms the bottom of the hydrophobic S4 binding site. The phenyl ring of the benzimidazole of **3b** is in close proximity to residues Tyr177, Asn97, and Lys98 at the base of the fIXa S4 pocket. In view of the differences in amino acid sequence in this region (i.e., the corresponding residues in fXa are Thr177, Glu97, and Thr98) and the more restricted conformation of the fIXa 99-loop,^{8b} more extensive SAR in this region may lead to improved selectivity.

In conclusion, we have identified several pyrazole compounds, which are potent dual inhibitors of fIXa and fXa, and have shown that the fIXa/fXa potency ratio can be modulated by changes to the P4 moiety as well as in the region where these molecules might interact with Glu219. The X-ray crystal structure of reversible inhibitor **3b** complexed with porcine fIXa provides additional structural insights, which can be used in the future design of more potent and selective fIXa inhibitors.

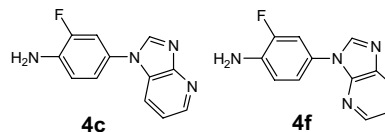
Acknowledgements

We would like to thank Dr. Chong-Hwan Chang for assistance with refinements of the final crystal structure for publication. We also thank Mr. Eugene Amparo and Mr. Michael Orwat for their synthetic assistance.

References and notes

- Kaiser, B. *Drugs Future* **1998**, *23*, 423.
- Himber, J.; Refino, C. J.; Burcklen, L.; Roux, S.; Kirchhofer, D. *Thromb. Haemost.* **2001**, *85*, 475–481.
- Feuerstein, G. Z.; Toomey, J. R.; Valocik, R.; Koster, P.; Patel, A.; Blackburn, M. N. *Thromb. Haemost.* **1999**, *82*, 1443–1445.

4. Pinto, D. J. P.; Orwat, M. J.; Wang, S.; Fevig, J. M.; Quan, M. L.; Amparo, E.; Cacciola, J.; Rossi, K. A.; Alexander, R. S.; Smallwood, A. M.; Luetzgen, J. M.; Liang, L.; Aungst, B. J.; Wright, M. R.; Knabb, R. M.; Wong, P. C.; Wexler, R. R.; Lam, P. Y. S. *J. Med. Chem.* **2001**, *44*, 566.
5. Factor IXa inhibition was assayed using human fIXa with a chromogenic substrate in the presence of ethylene glycol, as described by Sturzebecher, J.; Kopetzki, E.; Bode, W.; Hopfner, K.-P. *FEBS Lett.* **1997**, *412*, 295.
6. Factor Xa inhibition was assayed using human enzymes with a chromogenic substrate, as described by Kettner, C.; Mersinger, L.; Knabb, R. *J. Biol. Chem.* **1990**, *265*, 18289.
7. Bode, W.; Brandstetter, H.; Mather, T.; Stubbs, M. T. *Thromb. Haemost.* **1997**, *78*, 501.
8. (a) Brandstetter, H.; Bauer, M.; Huber, R.; Lollar, P.; Bode, W. *Proc. Natl. Acad. Sci. U.S.A.* **1995**, *92*, 9796; (b) Hopfner, K.-P.; Lang, A.; Karcher, A.; Sichler, K.; Kopetzki, E.; Brandstetter, H.; Huber, R.; Bode, W.; Engh, R. A. *Structure* **1999**, *7*, 989–996.
9. Hopfner, K.-P.; Brandstetter, H.; Karcher, A.; Kopetzki, E.; Huber, R.; Engh, R. A.; Bode, W. *EMBO J.* **1997**, *16*, 6626–6635.
10. Pruitt, J. R.; Pinto, D. J. P.; Galembo, R. A., Jr.; Alexander, R. S.; Rossi, K. A.; Wells, B. L.; Drummond, S.; Bostrom, L. L.; Burdick, D.; Bruckner, R.; Chen, H.; Smallwood, A.; Wong, P. C.; Wright, M. R.; Bai, S.; Luetzgen, J. M.; Knabb, R. M.; Lam, P. Y. S.; Wexler, R. *J. Med. Chem.* **2003**, *46*, 5298.
11. For example, the reaction of 2-fluoro-4-iodoaniline with 4-azabenzimidazole gave a roughly 60:40 mixture of the 4- and 7-azabenzimidazoles, **4c** and **4f**, which were separated by flash chromatography using a gradient elution from 0% to 3% MeOH in CH₂Cl₂.



12. Kipnis, F.; Levy, I.; Ornfelt, J. *J. Am. Chem. Soc.* **1948**, *70*, 4265.
13. Ashton, W. T.; Doss, G. A. *J. Heterocycl. Chem.* **1993**, *2*, 307.
14. The structure of porcine factor IXa complexed to **3a** was solved to 2.9 Å resolution with a crystallographic *R*-factor of 21.6%. Data were collected at DND-CAT at the Advanced Photon Source using synchrotron radiation. Coordinates of the factor IXa–**3a** complex have been deposited to the Protein Data Bank with code 1X7A. (Berman, H. M.; Westbrook, J.; Feng, Z.; Gilliland, G.; Bhat, T. N.; Weissig, H.; Shindyalov, I. N.; Bourne, P. E. The Protein Data Bank. *Nucleic Acids Res.* **2000**, *28*, 235).
15. Brandstetter, H.; Kuehne, A.; Bode, W.; Huber, R.; Wirthensohn, K.; Engh, R. A. *J. Biol. Chem.* **1996**, *271*, 29988.